

# Particle Physics in the LHC Era

G. Barr, R. Devenish, R. Walczak, T. Weidberg

January 7, 2015

# Accelerators

# 3

Accelerators are devices which accelerate charged particles to a broad range of energies from keV to TeV. This chapter is a very brief introduction to accelerators in particle physics or high energy nuclear physics. There are only a few accelerators used for particle or nuclear physics but they are about 30 000 accelerators used currently worldwide for other very important applications. There are about 9000 accelerators used in cancer therapy, 9500 in ion implantation<sup>1</sup>, 4500 for cutting and welding, 2000 for electron beam and X rays sources, 1000 for neutron generators and more in other fields. Depending on an application, accelerators are built using a technology most suitable for that particular application. In this very brief introduction we will focus only on synchrotrons and linear accelerators as those designs are typical choices in particle physics. Some excellent introductory textbooks on accelerator physics are given in the further reading section at the end of this chapter.

<b>3.1 Radio Frequency acceleration</b>	<b>47</b>
<b>3.2 Beam optics</b>	<b>53</b>
<b>3.3 Colliders and fixed targets</b>	<b>61</b>
<b>3.4 Luminosity</b>	<b>62</b>
<b>3.5 <math>\bar{p}p</math> Colliders</b>	<b>64</b>
<b>Chapter summary</b>	<b>66</b>
<b>Further reading</b>	<b>67</b>
<b>Exercises</b>	<b>67</b>

<sup>1</sup>An essential step in electronic chip fabrication.

## 3.1 Radio Frequency acceleration

Particles are accelerated by the electric field only

$$\mathbf{E} = -\nabla\varphi - \frac{\partial\mathbf{A}}{\partial t} \quad (3.1)$$

were  $\varphi$  is the scalar and  $\mathbf{A}$  the vector potential. In particle physics accelerators the time dependent vector potential  $\mathbf{A}$  is the source of the accelerating field  $\mathbf{E}$ . The simplest realisation is a cylindrical structure, sketched in fig 3.1, and is called a pill-box cavity. Microwave radiation (with frequency in the MHz-GHz range) produced in a device called a klystron (see sec 3.1.1) is guided to the pill-box cavity where it forms a standing wave; i.e. the pill-box cavity acts as a resonator. In free space, electromagnetic waves can only have transverse electric and magnetic fields with respect to the direction of propagation, however inside a cavity we can have Transverse Electric (TE) or Transverse Magnetic (TM) modes, indicating fields which have either longitudinal magnetic or electric fields respectively. Since we need a longitudinal electric field to accelerate charged particles, only the TM modes will be useful. The modes can be found by solving Maxwell's equations in free space without free charges or currents, subject to the usual boundary conditions at the conducting surfaces of the cavity. These conditions ensure that the longitudinal component of the E field and the perpendicular component of the  $\mathbf{B}$  field vanish at the surface of a conductor.

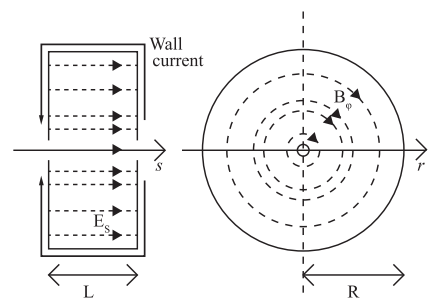


**Fig. 3.1** A pill-box cavity.

The useful (i.e. accelerating) modes of this cavity are  $TM_{nlm}$  where the indices,  $n, l, m$  refer to the field variations along the usual polar coordinates,  $\phi$  (azimuthal),  $r$  (radial) and  $z$  (longitudinal, i.e. along the beam direction). Since the radial variations are given by Bessel functions and we require non-zero component of the electric field in the longitudinal direction,  $s$ , on-axis (i.e.  $E_s(r=0) \neq 0$ ) and we must satisfy the boundary conditions at the surface of the conductor, we need the  $l=1$  modes. We want to select the modes which minimize the energy stored (and hence electricity costs) for a given accelerating gradient. This means we use the  $TM_{010}$  mode. This mode has only two components, the electric field  $E_s$  in the direction of the acceleration ( $s$ ) and the azimuthal component of the magnetic field  $B_\phi$  in the cavity (as indicated in fig 3.1) which are oscillating with the Radio Frequency (RF) frequency  $\omega$ :

$$E_s \sim J_0(kr) \exp(\omega t) \quad B_\phi \sim J_1(kr) \exp(i\omega t) \quad (3.2)$$

where  $J_0$  and  $J_1$  are the lowest order Bessel functions,  $k = 2\pi/\lambda$  is the wave number. The requirement that  $E_s(R) = 0$  where  $R$  is the radius of the pill-box, determines the allowed value of  $k$  from the zeroes of the Bessel function. Therefore for the  $l=1$  mode,  $\lambda \simeq 2.62R$ . The amplitudes  $J_0$  and  $J_1$  depend on the radial coordinate  $r$  as sketched in fig 3.2.

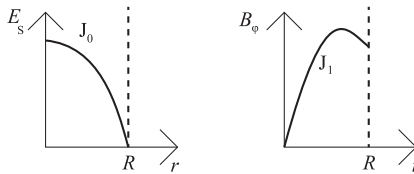


**Fig. 3.2** Amplitudes of the  $TM_{010}$  fields in a pill-box cavity.

<sup>2</sup>there will be straight sections, for example in the experimental halls where particle physics detectors are located.



**Fig. 3.3** The principle of synchronicity in a synchrotron.

<sup>3</sup>The groups of particles in filled buckets are called bunches. At the LHC the spacing between buckets is 2.5 ns but only  $\sim 10\%$  of buckets are filled with protons.

Suppose now that we want to accelerate protons in this pill-box cavity along the direction  $s$  which goes from left to right. We need to inject these protons into the cavity when the electric field component  $E_s$  can accelerate them, i.e. it is positive. After time  $t = \pi/\omega$  the field changes sign and injected protons would be decelerated. If we further assume that the pill-box cavity is an accelerating structure of a synchrotron where protons go around on a closed trajectory, approximately a circle<sup>2</sup>, then we will end up with the synchronicity condition

$$\omega = N\omega_{rev}; \quad (3.3)$$

The RF frequency needs to be an integer ( $N$ ) multiply of the revolution frequency  $\omega_{rev}$  with which protons go around in the synchrotron. This is demonstrated in a cartoon in fig 3.3. The value of  $N$  is chosen for practical reasons, e.g. to make the RF frequency lie in the range where components such as amplifiers are available. This means that  $N$  is typically very large, e.g. at LEP  $N = 31,320$ . This defines the number of ‘buckets’ for which we can potentially store stable beams. However we usually only want to inject particles into a much small number of buckets<sup>3</sup>. In a synchrotron, protons go through the accelerating cavities many times gaining energy at every passage. The magnetic field guiding them through the accelerator (see section 3.2) changes along with the acceleration keeping them on the same orbit.

One can combine many pill-box cavities stacking them one after another as sketched in fig 3.5. Protons are then accelerated in gaps between the drift tubes (see fig 3.5) when the accelerating electric field points in the right direction and then ‘hide’ inside the drift tubes, isolated from

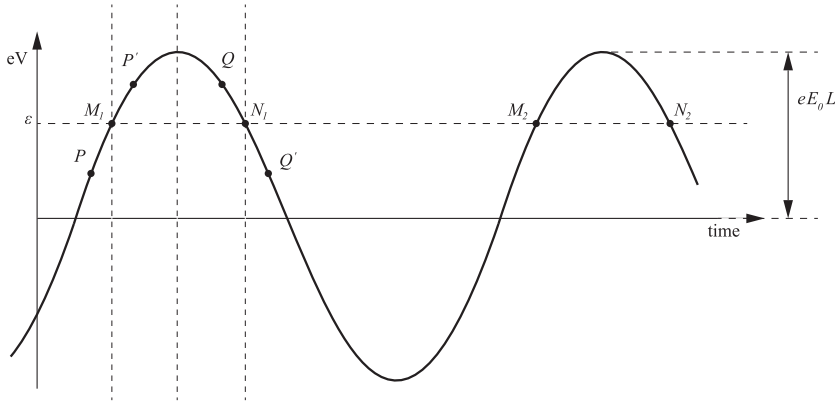


**Fig. 3.4:** Energy gain in a cavity as a function of the arrival time or relative phase of a beam particle with respect to the oscillating electric field in the cavity.  $E_0$  is the accelerating electric field amplitude,  $L$  the cavity length and  $e$  the charge of accelerated particle. Other symbols are explained in the text.

the electric field when it points the wrong direction, emerging in the next pill-box when the electric field is again pointing the right direction.

The fact that beam particles need to enter accelerating cavity at the right time leads to the bunch structure of the beam. This is demonstrated in fig 3.4 in more detail. A proton, for example, having nominal momentum  $p$ , traveling along the nominal path is called a synchronous particle and its trajectory is the reference trajectory. It arrives at the entrance to the cavity at point  $M_1$ . After going through the cavity its energy is increased by  $\varepsilon$  (here we are assuming that  $\omega L/c \ll 1$ ). Another proton arrives a little earlier at point  $P$  and its energy is increased by a smaller amount than  $\varepsilon$ , so when it enters the cavity again, after the next revolution, it will not be that early in comparison to the synchronous particle<sup>4</sup>. Yet another proton arrives a little late at point  $P'$ . This proton would gain more energy than  $\varepsilon$ , so after the next revolution, it won't be that late. In a synchrotron in which we combine the accelerating cavities with magnetic fields, these different energy gains and losses will lead to oscillations ('synchrotron oscillations'). In contrast, considering points  $Q$  and  $Q'$  in relation to point  $N_1$ , one can see that a proton arriving early with respect to  $N_1$  will gain more energy and that arriving late will gain less energy than the proton arriving at  $N_1$ , thus every revolution, considered protons would be further and further apart from each other, eventually escaping from the accelerator<sup>5</sup>. So  $M_1$  and  $M_2$  are stable points where bunches of beam particles can be located and  $N_1$  and  $N_2$  are unstable points.

The simplified discussion of phase stability need to be expanded to take into account competing changes: the speed of the particles and the radius of the orbit. The frequency is simply related to the speed  $v$  and

<sup>4</sup>For simplicity, we are assuming here that the paths around the accelerator are of the same length for all particles considered here. In reality different momenta/energies lead to different paths which need to be taken into account in addition.

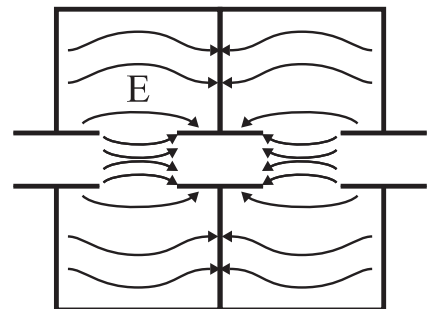


**Fig. 3.5** An accelerating cavity consisting of two pill-box cavities. A proton bunch in the left hand gap would be accelerated. A proton bunch in the middle drift tube would be shielded from the decelerating field. When it emerges into the right hand gap, the field has changed sign.

<sup>5</sup>Considering electrons one would need to take into account energy losses due

the radius  $R$  by

$$f = \frac{v}{2\pi R}. \quad (3.4)$$

Both  $v$  and  $R$  depend on the momentum of the particle. From relativistic kinematics we know that

$$p = \frac{mv}{\sqrt{(1-v^2)}}. \quad (3.5)$$

When the RF acceleration increases the momentum of the particle, it will also cause it to follow a slightly different orbit. This change in radius  $\Delta R$  is defined by the dispersion  $D$ , where for a certain change in momentum,  $\Delta p$  gives<sup>6</sup>

$$\Delta R = D \frac{\Delta p}{p}. \quad (3.6)$$

It is conventional to define the ‘slip factor’ which gives the fractional rate of change with frequency divided by the fractional change in momentum.

$$\eta_{rf} = \frac{\Delta f/f}{\Delta p/p}. \quad (3.7)$$

Substituting from eqn 3.5 and eqn 3.6 we can evaluate (see exercise 3.2) the two terms in eqn 3.7

$$\eta_{rf} = \frac{1}{\gamma^2} - \frac{D}{R_0} \quad (3.8)$$

where  $R_0$  is the radius of the reference trajectory. Therefore for injection at low momentum for which  $\gamma \sim 1$ , for a typical proton synchrotron  $\eta_{rf} < 0$ . However as the momentum increases, we will reach a transition in which  $\eta_{rf} = 0$  and for higher momentum,  $\eta_{rf} > 0$ . This implies that the region of phase stability flips when we cross the transition defined by

$$\frac{1}{(\gamma_{transition})^2} = \frac{D}{R_0} \quad (3.9)$$

<sup>6</sup>The value of the dispersion depends on the type and strength of the magnetic focusing. See Wilson in further reading for details.

Therefore we need to change the RF phase as we cross transition.<sup>7</sup> The concept of phase stability discussed here is one of the key ideas that enabled the successful operation of high energy accelerators.

For efficient operation of an accelerating cavity, i.e. a standing wave resonator, one requires that the energy is transferred from the resonator to the accelerated beam and not dissipated into the environment by losses to the walls of the cavity and radiation to the environment. This means that the  $Q$  value, i.e. the quality factor defined as the ratio of the average energy stored in the cavity ( $U$ ) to the average energy dissipated in one oscillation period ( $U_d$ ) is very large. The energy stored alternates between the electric and magnetic fields but we can calculate this from the peak value of the magnetic field ( $H_0$ )

$$U = (\mu_0/2) \int \mathbf{H}_0^2 d^3r \quad (3.10)$$

<sup>7</sup>This can be done sufficiently quickly that the particle losses are negligible.

We can calculate  $U_d$  from the Ohmic losses at the surface of the cavity<sup>8</sup>.

<sup>8</sup>This is a simplified calculation which neglects the radiation losses.

For a good conductor ( $\sigma/\epsilon\mu \gg 1$ ) we can neglect the displacement current. Using Amperè's law we can show that  $|\mathbf{H}| = j_s$  where  $j_s$  is the surface current per unit length. The power dissipated ( $I^2R$ ) can be evaluated as a surface integral

$$P = (1/2) \int \mathbf{H}_0^2 R_{surf} ds \quad (3.11)$$

where the surface resistance  $R_{surf} = 1/(\sigma\delta)$  and the skin depth  $\delta = \sqrt{(2/\mu\sigma\omega)}$ . The energy dissipated over one period  $T = 2\pi/\omega$ , is then given by

$$\Delta W = \pi \sqrt{\left(\frac{\mu}{2\sigma\omega}\right)} \int \mathbf{H}_0^2 ds \quad (3.12)$$

Comparing eqn 3.10 and eqn 3.12 we can see that to maximize the  $Q$  value we need a high frequency, high conductivity and a large volume to surface area ratio. The RF frequency used is usually in the range 100 MHz to  $\sim 10$  GHz.<sup>9</sup>

Next we need to consider the fact that the electric field is varying while the particle crosses the cavity. The electric field for the  $n = 0$  mode on axis ( $r = 0$ ) depends on time as

$$E_s = E_0 \cos(\omega t) \quad (3.13)$$

For an ultra-relativistic particle crossing the cavity the position along the axis of the cavity is simply  $z = ct$  and it's speed does not change but it gains energy over the length of the gap,  $G$

$$\Delta W = \int_{-G/2}^{G/2} E_0 \cos(\omega z/c) dz = \frac{\sin(\omega G/2c)}{\omega G/2c} E_0 G \quad (3.14)$$

From eqn 3.14 it is clear that for efficient acceleration, we need the gap length to be significantly less than the wavelength. This helps keep the bunches in the accelerating phase and prevents slippage into the decelerating phase. On the other hand we have seen that to obtain a high  $Q$ -value (and hence minimize Ohmic losses) we need a large ratio of volume to surface area. The actual shapes of RF cavities that are used in high energy accelerators have shapes optimized to meet these two requirements which include a short gap length and a large volume. A (very schematic) sketch of a cross section of a cavity is shown in figure 3.6 Typically many cavities are combined in one structure.

Good quality accelerating cavities which can be produced in large quantities have accelerating fields at the level of 20 to 30 MV/m. Single cavities might achieve up to 100 MV/m which is a breakdown limit (or beyond) for most materials.<sup>10</sup> To achieve larger accelerating fields, one needs a different approach. Fields up to 100 GV/m can be obtained in plasma (no walls to breakdown) where electrons can be displaced from quasi stationary ions. This is very active research area which eventually might lead to new generation of accelerators.

When charged particles are accelerated in a circular machine, they lose energy by synchrotron radiation. For an ultra-relativistic particle

<sup>9</sup>For superconducting cavities we have to consider the effective surface resistance, so there are still losses, however these are order of magnitudes smaller for superconducting Ni, compared to Cu which suffers from Ohmic losses.

<sup>10</sup>The breakdown mechanisms are different for conducting and superconducting cavities. For superconducting cavities, the hard limit is set by the fact that if the magnetic field at the surface becomes too large, the superconductor will return to the normal resistive state ('quench'). In practice no useful superconducting cavities have been made with gradients above 50 MV/m

of mass  $m$ , Lorentz factor  $\gamma$ , in an orbit with a radius of curvature  $\rho$ , the power emitted in the form of synchrotron radiation is

$$P = (2/3)r_c m \gamma^4 / \rho^2 \quad (3.15)$$

where  $r_c$  is the classical radius of the particle  $r_c = e^2 / (4\pi\epsilon_0 m c^2)$ . As the synchrotron radiation scales as  $\gamma^4$ , it will generally be negligible for protons, but the losses for electron machines will be very significant.

The energy loss grows as the fourth power of the energy, therefore there is a limit to the energy reach of circular electron machines. Although synchrotron radiation can be reduced by increasing the radius of the machine, this becomes prohibitively expensive at high energies. LEP is generally considered to be the highest energy circular electron accelerator that will be built and higher energy electron-positron machines will be linear colliders for which the synchrotron radiation is negligible<sup>11</sup>. While synchrotron radiation is a problem for particle physics applications, it turns out to have many uses in other areas of science. The synchrotron radiation in the laboratory frame is forward peaked around the electron direction and provides a very high brightness X-ray source. Dedicated electron rings are built with ‘wiggler’ magnets to increase the synchrotron radiation. The X-rays are used in condensed matter physics, biology, medical applications and other fields.

In a linear accelerator, one can use standing wave cavities as described above or one can use a traveling electromagnetic wave to accelerate electrons. Of course the traveling wave needs to be propagating in a waveguide like structure in order for the electric field to have a component along the travel direction. Then one can inject electrons to sit on the crest of that traveling wave and gain the energy as indicated in a cartoon in fig 3.7. A schematic sketch of an accelerating structure is shown in fig 3.8.

There are two approaches to particle acceleration. One is based on the use of cavities with short accelerating gaps (see eqn 3.14). An alternative approach uses a waveguide structure in which we have a traveling wave. However in a smooth waveguide the phase velocity is always larger than  $c$  and it therefore cannot be used for particle acceleration. One approach to this problem is to insert disks inside the structure that are used to adjust the phase velocity of the traveling wave. The radii  $a$  and  $b$  and the distances between disks are chosen such that the phase velocity of the wave equals the electron velocity. They need to be changing along the structure as electrons are being accelerated. But once the electrons’ speed becomes very close to the speed of light, there is no need for changing the geometry of the structure. A more realistic sketch of a structure is shown in fig 3.9. RF wave produced by a klystron enters and leaves each cavity to be absorbed outside the cavity. If instead of being absorbed the wave is reflected at the end of the cavity, a standing wave would be created which could be used to accelerate electrons as well.

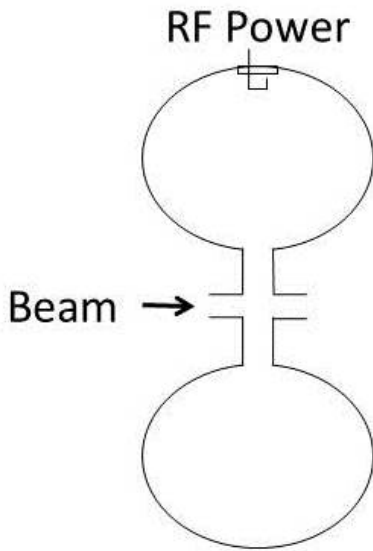


**Fig. 3.6** Schematic cross-section of an RF cavity (not to scale). Note the small accelerating gap and the relatively large volume. The RF power enters through an insulating ceramic window and couples into the cavity.

<sup>11</sup>There is currently some discussion about ideas for very larger circular colliders, including the  $e^+e^-$  option. If such a machine is ever built, it will certainly be very expensive!

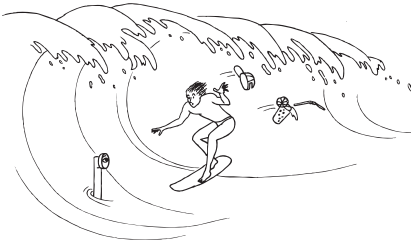


**Fig. 3.7** The principle behind traveling wave acceleration.

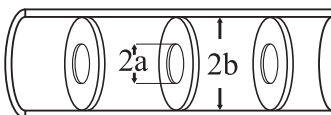


**Fig. 3.8** Disk-loaded accelerating structure.

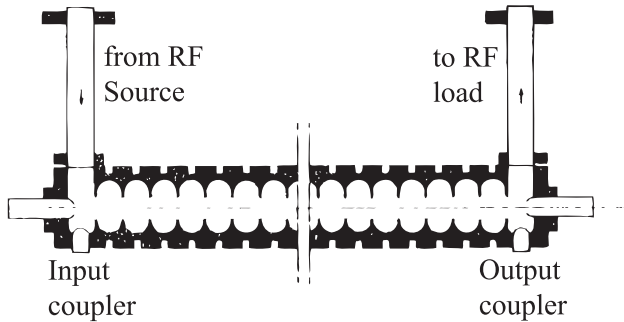


**Fig. 3.9:** Traveling wave accelerating structure.

### 3.1.1 Klystrons

This section gives a very brief and simplified idea of how klystrons work. A DC high voltage is first used to accelerate a continuous electron beam. The electron beam enters an RF cavity and RF power is delivered to the cavity at a resonant frequency. This causes the velocity of the electron beam to become modulated. The electrons enter a drift region in which the velocity modulation is translated into spatial modulation (bunching). Finally the electron bunches enter another RF cavity called the ‘catcher region’. They enter out of phase with the RF so they are decelerated and their kinetic energy is converted into the RF energy. The RF wave is then guided by a waveguide to the accelerating RF structure.

## 3.2 Beam optics

In order to guide and focus beam particles along the reference trajectory (which may not be a straight line), one needs magnets. In a synchrotron, for example, which has a circular geometry one needs dipole magnets providing a vertical magnetic field (the accelerators are constructed in the horizontal plane) to bend the trajectories of beam particles so they stay inside the beam pipe (with a good vacuum inside) close to the reference trajectory. But the vertical magnetic field is not enough. For example it does not constrain particle movement along the field direction so any vertical component of the momentum, however small, would result in beam particles eventually escaping the accelerator. One needs to have an arrangement of magnetic fields such that, beam particles are effectively confined as if they were in a potential well which prevents them from going too far away from the reference trajectory. Quadrupole magnets are needed for this plus other magnets for fine tuning. Only dipoles and quadrupoles will be considered here.

A schematic view of a dipole magnet is shown in fig 3.10. The beam pipe, a vacuum chamber, is placed in the yoke gap where a magnetic field  $B$  is created by electric currents in two coils. A ‘warm’ iron yoke can be used for fields up to about 2 T. To avoid iron saturation effects and achieve higher fields, one needs superconducting dipoles (see section 3.2.1). The radius of curvature  $\rho$  or the dipole bending strength

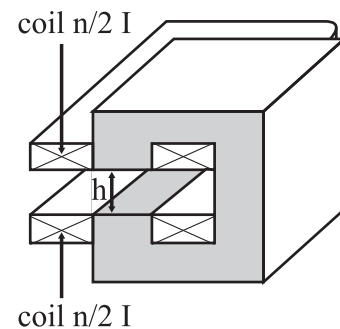


**Fig. 3.10** Schematic view of a dipole magnet.

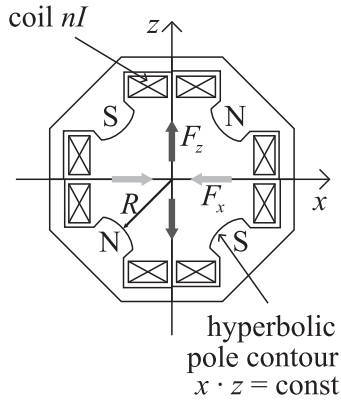


**Fig. 3.11** Schematic view of a quadrupole magnet.

<sup>12</sup>This equation assumes that we are not using a warm iron core magnet, i.e. it is valid for superconducting quadrupoles.

$1/\rho$  for a particle with momentum  $p$  and charge  $q$  is then

$$\frac{1}{\rho} = \frac{qB}{p} \simeq 0.3 \frac{B [\text{T}]}{p [\text{GeV}/c]} \text{ for } q = e = \text{the electron charge.} \quad (3.16)$$

In terms of the gap height  $h$ , the number of windings  $n/2$  and the current  $I$  in each coil,

$$B = \frac{\mu_0 n I}{h} \quad (3.17)$$

where  $\mu_0$  is free space permeability.

A schematic cross section of a quadrupole magnet is shown in fig 3.11.

Four pairs of coils, with  $n$  windings and the current  $I$  in each coil<sup>12</sup>, create the magnetic field with components  $B_x = -gz$  and  $B_z = -gx$  in the horizontal and vertical direction respectively where

$$g = \frac{2\mu_0 n I}{R} \quad (3.18)$$

and  $R$  is the distance shown in fig 3.11. The corresponding components of the Lorentz force acting on a particle with speed  $v$  are

$$F_x = qvB_z = -qvgx \text{ and } F_z = -qvB_x = qvgz. \quad (3.19)$$

The important point to note is that in the vertical plane (containing the origin, i.e. the reference trajectory point) the force is acting away from the origin and in the corresponding horizontal plane it acts towards the origin. One says that the quadrupole is focusing in one plane and defocussing in another plane, perpendicular to the first. There is a full analogy with geometrical optics and for a quadrupole of length  $l$ , with the quadrupole strength  $k$  one can define its focal length  $f$ :

$$\frac{1}{f} = kl \text{ where } k [\text{m}^{-2}] = \frac{qg}{p} \simeq 0.3 \frac{g [\text{T}/\text{m}]}{p [\text{GeV}/c]} \text{ for } q = e. \quad (3.20)$$

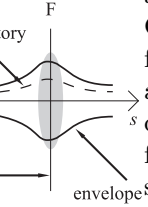
For the HERA proton ring,  $k \simeq 0.033 \text{ m}^{-2}$ ,  $l \simeq 1.9 \text{ m}$  and  $f \simeq 16 \text{ m}$ . If  $f \gg l$  the quadrupole can be treated as a thin lens irrespective of the absolute value of  $l$ .

A thin lens with the focal length  $f_1$  and another thin lens with a focal length  $f_2$  arranged as a doublet of lenses separated by a drift tube of distance  $l$  is a focusing doublet with an effective focal length  $f$  (see exercise 3.4) given by

$$1/f = 1/f_1 + 1/f_2 + l/f^2 \quad (3.21)$$

If one lens is focusing in the horizontal plane ( $f$  positive) and one defocussing ( $f$  negative) then we can arrange for the effective focal length of the system to be positive. Therefore a quadrupole doublet with a drift space between the two quadrupoles can be arranged to give focusing in both the horizontal and vertical directions. For example let  $f_1 = f_Q$  and  $f_2 = -f_Q$ , then the effective focal length is given by  $f = f_Q^2/l$  in both the horizontal and vertical dimensions. This is the idea behind

pective, the  
tube. Note  
effective focal



so called ‘strong focusing’: focusing and defocussing quadruples are arranged in doublets with a dipole inside each doublet<sup>13</sup>. A structure like this is called a FODO cell as sketched in fig 3.12. A FODO cell focuses beam particles in both planes. FODO cells are put together one after another as a periodic structure along the whole ring of a synchrotron. Calculations of particle trajectories inside such a structure can be performed using the same techniques as those used in geometrical optics and therefore this part of accelerator physics is called beam optics. The concept of using repeating structures of FODO cells is called ‘strong focusing’ and it keeps the transverse dimensions of the beam relatively small all the way around the ring, which allows for the use of relatively small beam pipes and magnets. Before strong focusing was discovered, synchrotrons used ‘weak focusing’ which resulted in much larger beam pipes. Therefore strong focusing was another key development that allowed the construction of very high energy synchrotrons at an affordable price.

The motion of beam particles is described in a curvilinear coordinate system, as sketched in fig 3.13. In a first, linear approximation, a particle motion in each of the three space directions, longitudinal  $s$ , vertical  $z$  and horizontal  $x$ , can be considered separately. The transverse phase space is split into two 2-dimensional phases spaces. Considering, for example, the vertical direction, we have the  $z$  coordinate and  $p_z$  component phase space. As indicated in fig 3.14, the velocity  $z$  component can be described as a product of the angle with respect to the  $s$  direction and the speed along  $s$  which is approximately the speed of light. So effectively, for a given and constant Lorentz  $\gamma$  factor, what matters is the angle and the  $z, p_z$  phase space can be replaced by  $z, z' = dz/ds$  phase space. A similar argument applies in the other transverse direction. The strength of a quadrupole is defined by

$$k = \frac{1}{B\rho} \frac{dB_z}{dx} \tag{3.22}$$

where  $\rho$  is the radius of curvature of the reference trajectory<sup>14</sup>. The eqns of motions are then (Hill’s equations)

$$z'' + k(s)z = 0 \tag{3.23}$$

$$x'' - (k(s) - \frac{1}{\rho^2})x = \frac{1}{\rho} \frac{\Delta p}{p}. \tag{3.24}$$

We will only consider solutions for  $z$  and  $z'$  (or for the horizontal phase space for  $\Delta p = 0$ , i.e. for the nominal momentum and at the limit of  $\rho \rightarrow \infty$ ). This differential equation is reminiscent of SHM but  $k(s)$  is not a constant but is a periodic function which defines the focusing strength at any point along the ring (eqn 3.22). If there was no focusing and  $k(s) = 0$  it is obvious that beam particles could escape unimpeded. If  $k(s)$  was constant around the ring, then the solution would be SHM. This suggests the use of an oscillatory trial function which looks similar to SHM<sup>15</sup>.

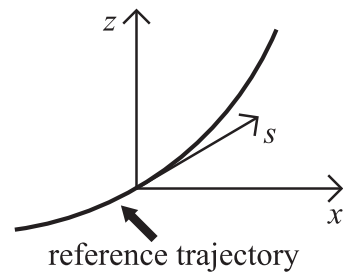


Fig. 3.13 Curvilinear coordinate system along the reference trajectory.

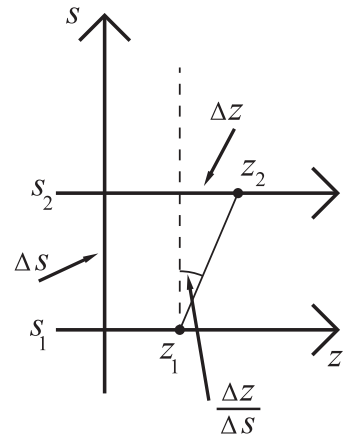


Fig. 3.14 A particle going from  $z_1$  to  $z_2$  in the vertical direction.

<sup>14</sup>In general as we go around a ring ( $s$ ) the magnetic focusing will vary, so we write  $k(s)$  to remind ourselves that  $k$  is not a constant.

<sup>15</sup>See exercise 3.3 for a justification.

$$\begin{pmatrix} z \\ z' \end{pmatrix} = \begin{pmatrix} \sqrt{\epsilon}\sqrt{\beta(s)} \cos(\varphi(s) - \varphi_0) \\ -\frac{\sqrt{\epsilon}}{\sqrt{\beta(s)}} [\sin(\varphi(s) - \varphi_0) + \alpha(s) \cos(\varphi(s) - \varphi_0)] \end{pmatrix}. \quad (3.25)$$

The initial conditions determine the values of  $\epsilon$  and  $\varphi_0$ . The function  $\beta(s)$  defines the amplitude modulation which varies because of the changing focusing strength around the ring. From our trial solution, we can also derive the relationship between the function  $\beta(s)$  and the magnetic focusing  $k(s)$ . It is convenient to define  $\beta = \omega^2$  and then we find (see exercise 3.3)

$$\omega'' - 1/\omega^3 + \omega k(s) = 0. \quad (3.26)$$

In principle this allows us to determine  $\omega(s)$  and hence  $\beta(s)$  if we know  $k(s)$ . However this is not practical and matrix methods are used to determine  $\beta(s)$  (see Wille in further reading). The phase advance function  $\phi(s)$  is also determined by the focusing. They resulting oscillations about the reference trajectory are called betatron oscillations. The amplitudes of  $z$  and  $z'$  are written using the amplitude function  $\beta(s)$  and the emittance  $\epsilon$  of the trajectory (at the moment we are talking only about one particle). The optical function  $\alpha(s) \equiv -\beta'(s)/2$  and the phase function  $\varphi(s)$  are related to the  $\beta(s)$  function by  $\varphi'(s) = 1/\beta(s)$  (see exercise 3.3).

In a given point  $s$  along the reference trajectory, a particle has  $z$  and  $z'$  coordinates in the vertical phase space. After one revolution, it would come back to the same  $s$  but with different  $z$  and  $z'$  coordinates every revolution they would be different tracing an ellipse as shown in fig 3.15. Integrating the phase function around the accelerator with the circumference  $C$ , one gets

$$\int_s^{s+C} d\varphi = 2\pi Q_z \quad (3.27)$$

where  $Q_z$  is known as the betatron tune, the number of betatron oscillations going around the accelerator (in this case the vertical tune  $Q_z$ ; similarly there is the horizontal tune  $Q_x$ ). If there are any small imperfections in a ring, we need to avoid particles crossing these imperfections at the same betatron phase in each revolution, otherwise the beam will rapidly ‘blow up’. Therefore integer values of the betatron tune should be avoided. In a more general form,

$$nQ_\nu + mQ_\mu = \xi \quad (3.28)$$

with  $\nu, \mu, \xi$  integers must be avoided.

The area of this ellipse is  $\pi\epsilon$  so, up to the factor of  $\pi$ , the emittance  $\epsilon$  is the volume of the 2-dimensional phase space (to be more precise, here  $\epsilon_z$  and similarly  $\epsilon_x$  for the horizontal phase space). Liouville’s theorem states that under the action of conservative forces the volume of beam phase space is conserved<sup>16</sup>. Therefore moving from one point  $s$  to another along the reference trajectory one would get another ellipse

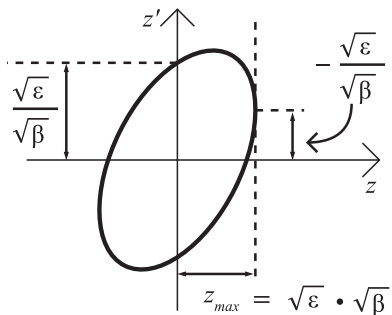


**Fig. 3.15** The phase space ellipse in the  $z - z'$  plane.

<sup>16</sup>We will see how to evade Liouville’s theorem when we consider stochastic cooling in sec 3.5.

but with the same area. So the transverse motion of a particle can be visualized as an ellipse of fixed area changing its shape depending of the location in the accelerator. If there is another particle in the accelerator which is described by the same equations of motion except the initial phase  $\varphi_0$ , the motion of that particle would be given by the same ellipse as changing  $\varphi_0$  corresponds to another point on the same ellipse. So, in fact, one ellipse describes a family of trajectories not just one. From the algebraic point of view this family of trajectories is described by the amplitude function  $\beta(s)$  and the emittance  $\epsilon$  (see eqn 3.25). But the emittance is constant for ‘coasting’ (no acceleration) beam particles and that means that we reduced the problem from two dimensions,  $z$  and  $z'$  to one dimension  $\beta$ . Inspecting fig 3.15, one can see that the amplitude function  $\beta(s)$  is the ratio of the beam width over the on-axis angular spread.

Each ellipse represents a family of particles and the whole ensemble of beam particles consists of many of these families and ellipses. How to represent the whole ensemble? Considering the vertical phase space (the same argument applies for the horizontal one) a particle beam injected into an accelerator is characterized by initial conditions, equivalent to a cluster of points in the  $(z, z')$  phase space, centred about the reference trajectory  $(0, 0)$ . One chooses an ellipse that closely surrounds this cluster and thus represents the “edge” of the beam. By convention, the ellipse should contain 95 % of particles. Then one follows this ellipse through the accelerator and this ellipse and the corresponding amplitude function  $\beta(s)$  and the beam emittance  $\epsilon$ , represent the properties of the whole beam.

Using Liouville’s theorem we see that as long as the beam is not accelerated,  $(z, z')$  and  $(z, p_z)$  phase spaces are equivalent. But once the beam is accelerated than Liouville’s theorem applies only to the proper phase space  $(z, p_z)$  and only the normalized emittance  $\epsilon_N = \beta\gamma\epsilon$  ( here  $\beta$  is the speed and  $\gamma$  is the Lorentz factor) is conserved. The volume of the  $(z, z')$  phase space shrinks with the momentum  $p$  as  $1/p$  and consequently, the beam width and the beam angular divergence shrink during the acceleration, each as  $1/\sqrt{p}$ ; so a higher energy beam fits into a smaller diameter beam pipe. This explains why high energy accelerators require chains of lower energy accelerators; each accelerator in the chain, reduces the emittance sufficiently to allow the beam to have sufficiently small emittance to fit into the next accelerator in the chain. In principle this accelerator chain could be eliminated if the beam pipe of the high energy accelerator were sufficiently large, however this would increase the size and hence costs of the magnets<sup>17</sup>.

### 3.2.1 Superconducting Magnets

The superconducting magnets are based on NiTi<sup>18</sup>. For the LHC dipoles [?], which are capable of generating a magnetic field  $B = 8.3T$ , the current required is  $I = 11.85 kA$ . This requires cooling the NiTi superconductor to a temperature of 1.9 K using superfluid He<sup>19</sup>. In a Type I supercon-

<sup>17</sup>An example of such a chain, is at the LHC [?] where the source of protons is a bottle of hydrogen gas. A high voltage is used to strip electrons to provide the protons. A linear accelerator (Linac 2) accelerates the protons to an energy of 50 MeV. The beam is then injected into the Proton Synchrotron Booster (PSB), which accelerates the protons to 1.4 GeV, followed by the Proton Synchrotron (PS), which accelerates the beam to 25 GeV. Protons are then injected into the Super Proton Synchrotron (SPS) where they are accelerated to 450 GeV before injection into the LHC.

<sup>18</sup>NiTi is the only low temperature superconductor which is ductile and hence most existing superconducting magnets are based on this alloy, although there is interest in NiSn which might be able to produce larger magnetic fields.

ductor the current only flows on the surface, not in the bulk which limits the useful magnetic field. Therefore high field superconducting magnets rely on Type II superconductors in which magnetic fluxoids can penetrate the volume. When there is a changing magnetic field in a superconductor, this will cause screening currents to flow. These are similar to eddy currents but as there is no resistance they do not decay with time. This magnetization appears as an unwanted error in the field produced by the magnet. The magnetization is proportional to the diameter of the wire carrying the current. When the magnetic field is changing with time as happens when the beam energy is being ramped up from injection energy, an additional magnetization is created from the flow of current between neighbouring filaments. Therefore a useful superconducting cable has to be made from a very large number of very small filaments<sup>20</sup>. For example the cable for the LHC dipole magnets [?] is based on 6  $\mu\text{m}$  diameter filaments. The filaments are embedded in a copper matrix for mechanical support (note that copper is effectively an insulator when the NiTi is in the superconducting state). 6300 filaments are used to make each strand which are 0.825 mm in diameter. 36 strands are then used to make a cable as shown in fig 3.16<sup>21</sup>.

<sup>20</sup>The filaments are wound as ‘twisted pairs’ to minimize the magnetization.

<sup>21</sup>For the same reasons as discussed above it is important to minimise the flux linkage between wires. Twisting wires around each other as in a conventional cable is not sufficient because the inner (outer) wires remain inside (outside). The wires need to be fully transposed, i.e. every wire must change places with every other wire along the length of the cable so that, averaged over the length, no flux is enclosed. This type of cable is called Rutherford cable as it was developed at the Rutherford Laboratory, and is used in all high field superconducting magnets. These cables are used in MRI scanners, so this is probably one of the most important but least known spin-offs from particle physics research.

<sup>22</sup>This also allowed for significant cost savings compared to having two separate magnets and cryostats.

<sup>23</sup>An additional source of danger is the electrical connection between the dipoles. This has a tiny but non-zero resistance. If this resistance is too large, this can also lead to catastrophic thermal runaway as occurred on the 19th September 2008, which led to extensive damage. Many improvements have been made since then to prevent this type of problem.

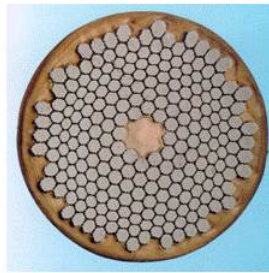
To create a perfect dipole field, a distribution of current density varying as  $\cos\phi$  around the beam pipe would be required. However a very nearly uniform dipole field near the centre of the beam pipe is created by blocks of superconductor arranged in the geometry shown in fig. 3.16(d). The currents in the blocks are optimized to produce a uniform magnetic field. As there was insufficient space in the LHC tunnel for separate magnets for each beam, a ‘two-in-one’ magnet was designed in which the two magnetic volumes are inside a common cryostat [?]<sup>22</sup> as illustrated in fig. 3.17. The superconducting cable is held in place by non-magnetic ‘collars’ of austenitic steel, which can withstand the magnetic force of about 400 tonnes per metre of dipole. At nominal operation, the energy stored in each of the 1232 LHC dipoles is 6.93 MJ. If one small region of the superconductor becomes non-superconducting (called a quench) for any reason, there will be Joule heating, which will increase the resistance and hence there is the possibility of a catastrophic run away which would destroy the magnet. Therefore sophisticated quench detection and protection systems are essential. Quenches can be detected by the extra ‘IR’ voltage drop. Once a quench is detected a ‘quench heater’ is operated to force the entire magnet to become non-superconducting and the energy is transferred to a large ‘dump’ resistor<sup>23</sup>.

The energy stored in the two beams at nominal operation is 362 MJ. The beams therefore have sufficient energy to destroy large parts of the LHC machine and the detectors. Therefore many beam loss monitors are installed in the machine and if the rates are above a threshold, kicker magnets are operated to deflect the beams out of the ring towards a beam dump [?].

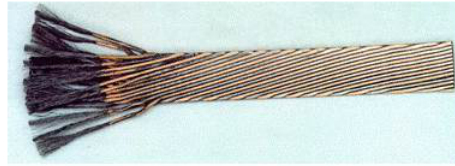
(a) filament



(b) strands



(c) cable



(d) dipole

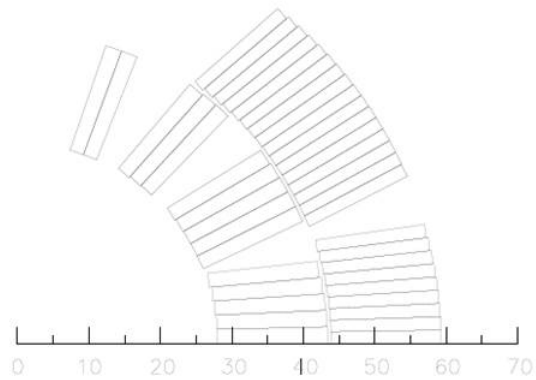


**Fig. 3.16:** Filaments (a), strands (b), cable (c) of the type used for the LHC superconducting magnets and a cross section of one quarter of the coils used in a main dipole (d).

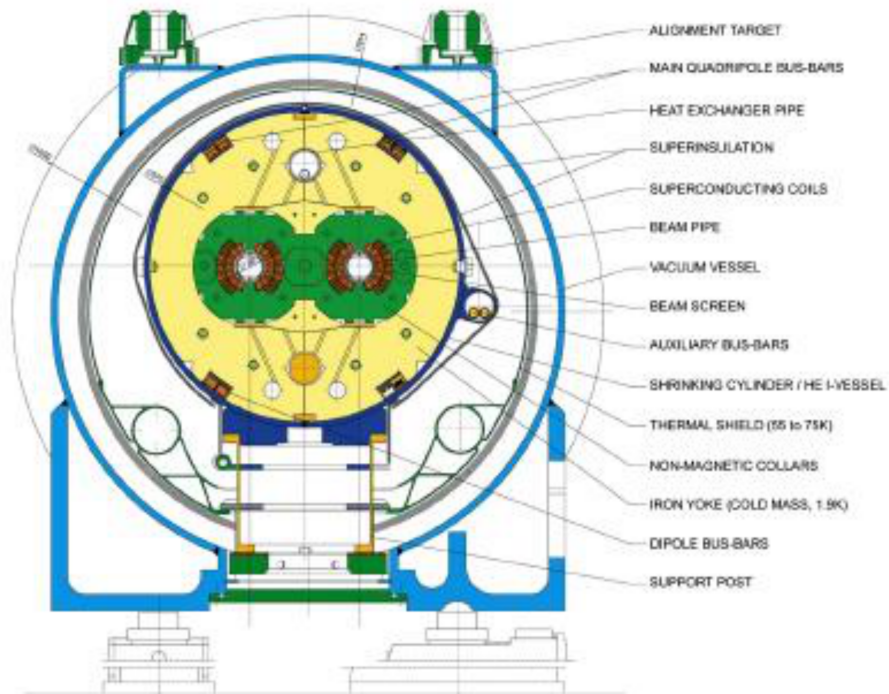


Fig. 3.17: Cross section of an LHC dipole in it's cryostat.

### 3.3 Colliders and fixed targets

The centre of mass energy in a symmetric collider, with each beam having energy  $E$  is simply given by  $\sqrt{s} = 2E$ . For a fixed target collision, with a beam energy  $E$  and a target mass  $m$  (assuming  $E \gg m$ ) we can show (see problem 3.1) that

$$\sqrt{s} = 2mE \quad (3.29)$$

Therefore colliders have an obvious advantage in achievable centre of mass energies over fixed target experiments. Although this was realized a long time ago, the challenge of achieving a useful interaction rate was formidable. The interaction rate for a given physics process depends on the luminosity (see 3.4). In a fixed target geometry one only needs one high intensity beam to collide with a block of matter to achieve very high luminosities. Any collider is far more challenging because we need two intense beams, which both have to be focused to very small transverse dimensions at the interaction points to achieve a useful luminosity. In a fixed target accelerator, one only needs to keep the beam for a few seconds before it is extracted. However in a collider it takes time to ‘fill’ the machine with sufficient numbers of particles before they are accelerated to the peak energy and then the beams have to be kept for several hours while data is taken. Accelerators!colliding beam experiments This obviously puts much more significant demands on the quality of the accelerator. We need to be extremely careful to avoid the dangerous resonances and the quality of the machine has to be much higher to avoid the imperfections increasing the emittances of the beams. We also need an extremely high vacuum to minimize beam losses and backgrounds in the detector<sup>24</sup>. There can also be important defocussing effects of one beam on the other.

Some of the issues for colliders are common to all types of colliders. We always want more luminosity and how to achieve this is discussed in section 3.4. The special issue for circular  $e^+e^-$  colliders is synchrotron radiation (see eqn 3.15) and this puts a practical limit on the beam energy. Therefore large  $e^+e^-$  colliders like LEP have simple (and cheap) magnets but require very efficient RF cavities. This requires superconducting RF cavities (see sec 3.1). Hadron colliders do not suffer from significant synchrotron losses, so we can have much higher beam energies. In order to optimize the beam energy for a given cost, we need to use the highest magnetic field possible for the dipole bending magnets. The critical technology challenge is the industrial scale production of very high quality superconducting magnets (see sec. 3.2.1). In an  $e^+e^-$  collider, the energy defines what processes can be studied<sup>25</sup> and which particles can be created/discovered. In a hadron collider such as the LHC, there is a more subtle interplay between energy and luminosity. In a hadron collider we are really interested in the rates for processes at the parton level, and the partons only carry a fraction of the momentum of the protons. Therefore the energy reach of a hadron collider depends crucially on both energy and luminosity. Therefore there is

<sup>24</sup>At the LHC the vacuum the pressure has to be kept below about  $10^{-7}$  Pa.

<sup>25</sup>Energy conservation implies that for a beam energy  $E$ , in a symmetric collider, the most massive particle that can be pair produced would have mass  $m = E$ . In general the sum of the masses of the final state particles must be less than the centre of mass energy ( $2E$ ).

some complementarity between the very clean physics that can be performed at  $e^+e^-$  colliders, compared to the higher energy reach of hadron colliders, in which the event reconstruction is more complicated because in addition to the interesting parton-parton collisions, there are always interactions of the remaining ‘spectator quarks’.

The HERA collider was a special case because it used  $e^{+/-}p$  collisions. This required a high energy proton ring (HERA I 820 GeV, HERA II 920 GeV) and a much lower electron ring (27.5 GeV) to minimize synchrotron radiation.<sup>26</sup> As will be discussed in chapter 9 this gave the most precise determination of the quark and gluon distribution functions. These are required for all calculations of cross sections at hadron colliders like the LHC, the details will be covered in the same chapter.

The LHC uses  $pp$  collisions but earlier hadron colliders used  $\bar{p}p$  collisions. This important advantage of  $\bar{p}p$  colliders is that it allows for the two beams to be contained in the same beam pipe. The critical issue for these colliders was how to produce intense and low emittance  $\bar{p}$  beams. This will be discussed in sec 3.5. Colliders have also been operated using heavy ions but these will not be discussed in this book.

<sup>26</sup>The ep CM energies are 300, 318 GeV respectively.

### 3.4 Luminosity

The two most important numbers in experimental (accelerator) particle physics are: the energy and the luminosity of an accelerator. and the luminosity determines the rate for a given process; The luminosity  $\mathcal{L}$  translates a cross section  $\sigma$  into the number  $N$  of produced (observed if detector effects are included) events:

$$\frac{dN}{d\Omega} = \mathcal{L} \frac{d\sigma}{d\Omega} \quad (3.30)$$

where  $\Omega$  is the solid angle as an example of the differential cross section argument. In fixed target experiments

$$\mathcal{L} = n\rho l \quad (3.31)$$

where  $n$  is the number of particles per second in the beam (typically  $10^{12}\text{s}^{-1}$ ),  $\rho$  is the density of target particles and  $l$  is the target length (typically  $\rho l \simeq 10^{23}\text{cm}^{-2}$ ) giving a typical luminosity  $\mathcal{L} \simeq 10^{35}\text{cm}^{-2}\text{s}^{-1}$  which is large in comparison to typical numbers at high energy colliders although such luminosities can be reached by some of them<sup>27</sup>.

We begin by deriving useful formulae for the luminosity of colliders and then discuss how to optimize it. We first consider a very simple situation as sketched in fig 3.18. There are two rectangular bunches of particles colliding head on. They have, correspondingly,  $n_1$  and  $n_2$  randomly distributed particles.  $A$  is the transverse area of the wider bunch. There are  $b$  bunches in each beam and the frequency of revolution is  $f$ . Then

$$\mathcal{L} = \frac{n_1 n_2}{A} b f. \quad (3.32)$$

<sup>27</sup>This simple formula assumes that the target is ‘thin’, i.e. the probability that an individual beam particle interacts in the target is much less than one.

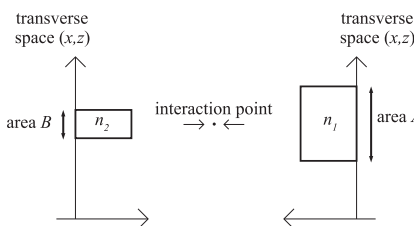


**Fig. 3.18** Simple geometry for luminosity formula derivation. Symbols are explained in the text.

In a collider  $n_2/A$  corresponds to the fixed target  $\rho l$ ; it is the number of target particles per unit area.

If particles are distributed in colliding bunches not randomly but according to normalized density distributions  $\varrho_1$  and  $\varrho_2$  then

$$\mathcal{L} = bf n_1 n_2 \int_s \varrho_1 \varrho_2 ds \quad (3.33)$$

where  $s$  is the transverse space.

Introducing beam currents,  $I_1 = n_1 e f b$  and  $I_2 = n_2 e f b$  where  $e$  is the electron charge,

$$\mathcal{L} = \frac{I_1 I_2}{e^2 b f} \int_S \varrho_1 \varrho_2 ds. \quad (3.34)$$

Assuming Gaussian distributions with  $\sigma_x = \sigma_z = \sigma$  for simplicity (this is not very realistic as typically the horizontal beam size is bigger than the vertical one)

$$\rho_{1,2} = \frac{1}{2\pi\sigma_{1,2}^2} \exp\left(\frac{-r^2}{2\sigma_{1,2}^2}\right) \quad (3.35)$$

we get

$$\mathcal{L} = \frac{I_1 I_2}{e^2 b f} \frac{1}{2\pi(\sigma_1^2 + \sigma_2^2)} \quad (3.36)$$

where  $2\pi(\sigma_1^2 + \sigma_2^2)$  represents an effective area.

In order to illustrate how this relates to the accelerator parameters, we will assume that the vertical and the horizontal emittances are equal  $\epsilon_x = \epsilon_z = \epsilon/\pi$  and that the horizontal and the vertical beta functions are equal  $\beta_x = \beta_z = \beta^*$ . The star in  $\beta^*$  is the common symbol to indicate that the function is calculated at the interaction point (IP). As

$$\sigma_x = \sigma_z = \frac{\epsilon\beta^*}{\pi} = \sigma^2, \quad (3.37)$$

$$\mathcal{L} = \frac{I_1 I_2}{e^2 b f} \frac{1}{\beta_1^* \epsilon_1 + \beta_2^* \epsilon_2}. \quad (3.38)$$

Eqn 3.38 gives the best guide to understand how to maximize the luminosity for a collider. Firstly it is clear that increasing the beam currents ( $I_1$  and  $I_2$ ) is desirable. If a limited number of protons can fit in one bunch, then it is advantageous to increase the number of bunches. However the beam currents cannot be increased indefinitely because each beam exerts electromagnetic forces on the other beam at each IP. The net effect of one bunch on a counter-rotating bunch is similar to that of an additional quadrupole magnet which therefore changes the horizontal and vertical Q-values<sup>28</sup>. This is very dangerous because even if the operating point of the machine is away from integer resonances (see eqn 3.28), such a tune shift can push the beams too close to a resonance and the result is very rapid beam loss. This beam-beam tune shift then limits the ultimate luminosity that can be achieved in a hadron collider<sup>29</sup>. Note the rather counter-intuitive result of eqn 3.38 that if the beam currents are at the beam-beam limit, then the luminosity can be increased by decreasing the number of bunches. However

<sup>28</sup>The effect is called the ‘beam-beam’ tune shift. See Wylie in further reading for a full explanation.

<sup>29</sup>The situation is different in  $e^+e^-$  colliders because of the beam ‘cooling’ from synchrotron radiation.

the optimization of the number of bunches also has to consider practical constraints imposed by the detectors. If the number of bunches are reduced, the number of collisions per bunch crossing will increase. Therefore collisions with one interesting event will also contain a background of many other ‘minimum bias’ collisions, which are effectively a noise source. There is therefore a trade-off between maximizing luminosity and having clean enough events to be useful and there is no perfect solution. At the LHC design luminosity of  $10^{34} \text{cm}^{-2} \text{s}^{-1}$  there will be approximately 25 collisions per bunch crossing (every 25 ns).

The next parameters to optimize are the emittances. These depend on the quality of the proton source. Although Liouville’s theorem predicts the conservation of beam phase space, any imperfections can increase the emittances. Finally one can increase the luminosity by decreasing the values of  $\beta^*$ . This is achieved by using very strong focusing quadrupole magnets, which will usually be superconducting to achieve the highest field gradients. The consequence of reducing the transverse beam at the IP is that the beam divergences will increase. This results in a limit in how far  $\beta^*$  can be reduced before the beam losses from particles hitting the beam pipe will become unacceptable. This implies that there is an advantage in bringing the quadrupole magnets closer to the IP but this will reduce the space for detectors in the forward region and the trade-off will depend on the particular physics being studied.

### 3.5 $\bar{p}p$ Colliders

Hadron colliders can use two separate  $p$  beams as in the LHC. However this requires two separate magnetic fields for the counter-rotating  $p$  beams. Using counter rotating beams of particles and antiparticles the electric and magnetic fields are automatically correct for both beams, so only one ring is required. This allowed for the relatively cheap conversion of proton synchrotrons at CERN and Fermilab into  $p\bar{p}$  colliders. The use of  $\bar{p}p$  colliders was very important as it led to the discovery of the  $W$ ,  $Z$  and top quark as well as providing the most precise measurement of the mass of the  $W$  boson<sup>30</sup>.

The big challenge for  $\bar{p}p$  colliders was to produce very intense, low emittance, beams of anti-protons, which was achieved using the technique of stochastic cooling [?]. Liouville’s theorem prevents a reduction in beam phase space but it is based on the assumption that the beam is continuous, whereas a real beam is composed of a finite number of discrete particles. Consider first the extreme case of a single particle in a beam; we can detect its transverse position using a beam pick up electrode at one place in the ring, which generates a signal proportional to the displacement about the central orbit. The signal is fed across the ring via an amplifier to two deflecting plates as shown in fig. 3.19.

The betatron function at the deflecting plates is an odd multiple of  $\pi/2$  out of phase with that of the pickup, so that a deviation in position from the reference orbit is converted to a difference in angle. The shorter path

<sup>30</sup>They also demonstrated to skeptical physicists that very clean results could be obtained in this difficult environment.

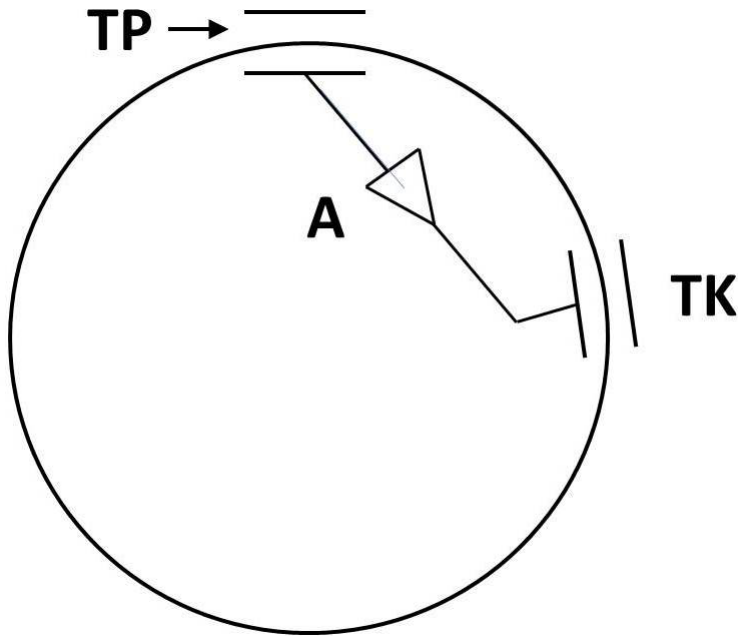


**Fig. 3.19:** Schematic view of a synchrotron with transverse pickup (TP), fast amplifier (A) and transverse kicker (TK) electrodes for stochastic cooling.

for the cable compared to the particle, compensates for the difference in speeds of the particles and the electrical signals as well as the delay in the amplifier. Therefore a suitable voltage pulse can be used to make a correction to bring the particle back to the central orbit.

In a real beam with a large number of particles, this cooling technique works on a statistical basis. If the speed of the amplifier were sufficiently fast then each individual particle in the beam would have the correction applied to bring it back to the central orbit. Therefore the cooling works better the shorter the sample time of the amplifier, as this determines how many particles are affected. Hence the cooling rate depends on the bandwidth of the amplifier  $W$ . As this stochastic cooling requires the detection of fluctuations it works faster for smaller number of beam particles  $N$  and the cooling time  $\tau \approx N/2W$ . For useful bunches we need  $N \approx 10^{12}$  and with achievable bandwidth amplifiers, this leads to a cooling time of the order of 1 day. It is also necessary to provide momentum cooling to reduce the spread in momenta. A pickup electrode can be used to measure the revolution frequencies of particles and the signal is fed into an amplifier via a filter. The filter eliminates any signal for particles with the correct frequency (i.e. momentum) and higher frequencies give a phase shift of  $\pi$ . This filtered signal can then be fed into an accelerating cavity. Again this system would work perfectly for individual particles and works on a statistical basis for beams with a finite number of particles.

### 3.5.1 CERN $\bar{p}p$ Collider

The antiprotons were produced by collisions of 26 GeV/c protons from the CERN PS with a copper target. Some of the produced antiprotons with momenta  $\sim 3.5$  GeV/c were collected by a large aperture low energy ring called the antiproton accumulator. The pulse of antiprotons was first cooled and then moved to the side of the aperture where the intense stack of antiprotons was built up, allowing a new injection of antiprotons every 2.2 s. The antiprotons were accumulated and cooled using stochastic cooling for about one day and then injected back into the PS and accelerated to 26 GeV/c and then injected into the SPS together with counter rotating bunches of protons. The protons and anti-protons were then accelerated up to an energy of 315 GeV (initially 270 GeV) and a run would last until sufficient anti-protons had been accumulated, or the beams were lost. The peak luminosity achieved was  $\sim 2 \cdot 10^{30} \text{cm}^{-2}\text{s}^{-1}$ .

### 3.5.2 Tevatron $\bar{p}p$ Collider

Similar principles were applied for the Tevatron. For the second phase of the Tevatron collider (run 2), a 150 GeV synchrotron called the main injector was built to provide higher yields of antiprotons. The acceptance of antiprotons and the cooling was split into two separate machines. After cooling the protons and antiprotons were reaccelerated in the main injector and then injected into the superconducting Tevatron and accelerated to an energy of 0.98 TeV. The peak luminosity achieved was  $\sim 10^{32} \text{cm}^{-2}\text{s}^{-1}$ .

## Chapter summary

- This chapter has given a brief introduction to the field of accelerator physics.
- We have seen how RF cavities are used to accelerate charged particles.
- Dipole magnets are required for circular machines but quadrupoles are also essential for beam focusing. The oscillations of beam particles about their central orbit are explained and beam emittance is defined.
- Superconducting cables are needed for the highest energy synchrotrons such as LHC.
- Colliders are the best route to the highest energy collisions, provided sufficient luminosity can be achieved. A brief explanation of luminosity and its optimization is given.
- How to beat Liouville's theorem with stochastic cooling is reviewed. This was essential for the operation of  $\bar{p}p$  colliders.

## Further reading

E. Wilson, *An introduction to Particle Accelerators*, OUP, 2001. A very good introduction to the subject.

P. Bryant and K. Johnsen, *The Principles of Circular Accelerators and Storage Rings*, Cambridge University Press, 1993.

K. Wilie, *The Physics of Particle Accelerators, an intro-*

*duction*, Oxford, 2000. A more advanced introduction to the subject.

The Staff of the CERN proton-antiproton project, *First proton-antiproton collisions in the CERN SPS collider*, Phys. Lett. 107b (1981) 306.

## Exercises

(3.1) Use relativistic kinematics to derive eqn 3.29.

(3.2) (a) using the definition in eqn 3.7, show by partial differentiation that

$$\eta_{rf} = \left( \frac{\partial f}{\partial v} \frac{\partial v}{\partial p} + \frac{\partial f}{\partial R} \frac{\partial R}{\partial p} \right) \frac{p}{f}$$

(b) Show that

$$\frac{\partial v}{\partial p} = \frac{1}{m\gamma^3}$$

(c) Combine the results from parts (a) and (b) to derive eqn 3.8.

(3.3) (a) Differentiate twice the trial solution of Hill's equation ( 3.25) in the  $z$  direction.

(b) Using the requirement that the coefficients of sin and cos must be identical and the results from (a) show that our trial solution to eqn 3.24 is valid provided we satisfy the condition  $\phi' = 1/\beta$ . (c) Verify eqn 3.26 by equating coefficients of the cos terms in Hill's equation ( 3.24).

(3.4) (a) Write down the matrices in the vertical direction ( $z, z'$ ) for a thin focusing (F) and de-focusing (D) lens and a drift tube (O) (i.e. with no magnetic forces). (b) Use matrix multiplication to evaluate the matrix for the combination FOD and hence derive eqn. 3.21.

(3.5) Consider the quadrupole magnetic field given by  $B_x = -gz$  and  $B_z = -gx$ . Show that this field satisfies Maxwell's equations in free space. Sketch the resulting magnetic field lines. Hence sketch the

magnetic forces acting on a positive particle travelling parallel the beam axis ( $s$ ). Consider the trajectory of a such a particle after traversing such a thin quadrupole lens of length  $l$ . The particle has an initial horizontal coordinate  $x = x_0$ . Show that all such particles will have  $x = 0$  after travelling a distance given by the focal length (eqn. 3.20). Hint: assuming the lens is thin, you may neglect the change in  $x$  of the particle inside the quadrupole.

(3.6) A collider with two beams of unequal width has  $3 \times 10^{11}$  particles per bunch, 2 bunches in each beam and the frequency of revolution is 1 MHz. Particles are uniformly distributed in cylindrical bunches which move parallel to the cylinder axis. The radius of each bunch in the wider beam is  $4 \times 10^{-4}$  m. Calculate the luminosity.

(3.7) Describe a method to determine the luminosity in an  $e^+e^-$  collider and explain what detectors you would need. Why can not this technique be used in a hadron collider?

(3.8) This question is about the measurement of luminosity at a  $pp$  collider such as the LHC using Van der Meer (VDM) scans. Consider a collider with a revolution frequency  $f_{rev}$  and  $n_b$  colliding bunches. Let the number of particles in beam 1(2) be  $n_1(n_2)$  and let the normalised bunch density be  $\rho_1(x, y)$  ( $\rho_2(x, y)$ ). The luminosity is defined by the interaction rate for a process with a given cross section  $\sigma$  by  $R = L\sigma$ . In terms of the beam parameters, the luminosity is expressed by

$$L = n_b f_{rev} n_1 n_2 \int \rho_1(x, y) \rho_2(x, y) dx dy \quad (3.39)$$

Explain the origin of this equation. Assume that the particle densities are uncorrelated in the  $x$  and  $y$  directions. The luminosity can then be written as

$$L = n_b f_{rev} n_1 n_2 \Omega_x \Omega_y, \quad (3.40)$$

where the beam overlap is defined in  $x$  (with an equivalent definition in  $y$ ) as

$$\Omega_x = \int \rho_1(x) \rho_2(x) dx \quad (3.41)$$

Assume that the beams have Gaussian distributions with a common centre and an RMS of  $\sigma_{x1}$  ( $\sigma_{x2}$ ). Show that

$$\Omega_x = \frac{1}{\sqrt{2\pi}(\sigma_{x1}^2 + \sigma_{x2}^2)^{1/2}}. \quad (3.42)$$

Let  $R(x)$  be the interaction rate as a function of the separation of the beams in the  $x$  direction.  $R(x) \propto \exp \frac{-x^2}{2(\sigma_{x1}^2 + \sigma_{x2}^2)}$ . Therefore the value of  $(\sigma_{x1}^2 + \sigma_{x2}^2)$  can be determined from a VDM scan if the interaction rate for some particular process  $R(x)$  is measured as the separation between the two beams  $x$  is varied. Assume that the fraction of bunch crossings which register a hit in a counter is  $p$ , show that the mean number of collisions which

produce such hits is given by  $\mu = -\ln(1-p)$ . Why is it advantageous to use a small counter? What is the problem with this technique at very high luminosity? Suggest a possible detector technique that could be used for such a counter?

(3.9) Synchrotrons have a periodic ring-shaped lattice of focusing and bending magnets. Specifying the position of a beam particle on the circumference of the accelerator by the distance  $s$ , the equations of motion in both horizontal and vertical directions about the ideal orbit have the form

$$\frac{d^2x}{ds^2} + K(s)x = 0, \text{ where } K(s+L) = K(s) \text{ is periodic.}$$

The solution is a quasi-periodic function of the form

$$x(s) = \sqrt{\varepsilon \beta(s)} \cos(\phi(s) - \phi_0), \text{ where } \varepsilon \text{ and } \phi_0 \text{ are constants.}$$

Both  $\varepsilon$  and  $\beta(s)$  have dimensions of length. The phase  $\phi(s)$  is related to the beta function  $\beta(s)$  by  $d\phi/ds = 1/\beta$ . Explain the significance of the beta function.

Show that  $x$  and  $x' \equiv dx/ds$  satisfy

$$\frac{x^2 + (\beta(s)x' + \alpha(s)x)^2}{\beta(s)} = \varepsilon, \text{ where } \alpha(s) = -\frac{1}{2} \frac{d\beta}{ds}.$$

Reduce the expression to the standard form for an ellipse in  $x - x'$  space and show that its area is  $\pi\varepsilon$ . This is the emittance of the beam (in one transverse direction). Explain its importance for accelerator design and control.